

### References

1. For a summary; Rhee, Jk. Ph. D Thesis, University of Washington (1989).
2.  $\text{PGH}_2$  is a known inducer of platelet aggregation. Its half life in aqueous solution is 5-30 min.
3.  $\text{TXA}_2$  is the product formed from  $\text{PGH}_2$  by the action of Thromboxane Synthase. It decomposes to inactive  $\text{TXB}_2$  in aqueous solution.
4. "Modern Pharmacology", second edition: Craig, Charles R., Stitzel, Robert E.
5. (a) P. Neediman, and S. Moncada, *Nature (London)* **261**, 558 (1976); (b) S. Moncada, P. Neediman, S. Bunting, and JR Vane, *Prostaglandins*, **12**, 323 (1976).
6. (a) T. Yoshimoto, S. Yamamoto, M. Okuma, and O. Hayashi, *J. Biol. Chem.*, **252**, 5871 (1977); (b) S. Hammarstrom and U. Diczfalusy, *Adv. Prostaglandins and Thromboxane Research* **6**, 267 (1980).
7. M. Haurand and V. Ullrich, *J. Biol. Chem.* **260**, 15059 (1985).
8.  $\text{PGE}_2$  shows two different functions depending on the concentration. At low concentration, it promotes aggregation induced by other agents (ADP, Arachidonic acid, etc) while, at high concentrations, it inhibits aggregation. It has now been shown to be an effector of TX-SYN (unpublished results, Andersen, NH, Rhee, Jk.) increasing the production of  $\text{TXA}_2$  from  $\text{PGH}_2$  at very low concentrations.
9. V. Ullrich, M. Haurand, *Adv. Prostaglandin Thromboxane Leukotrienes Research* **11**, 105 (1983).
10. p-Carboxyphenoxy-N-ethyl imidazole.
11. The basic structural requirements for selective inhibitor are a 1-imidazolyl or 3-pyridyl moiety at one end of the molecule and a carboxylic acid group at the other. Further the distance between the carboxylic group and the nitrogen atom at the 3 position or in the pyridine moiety should be between 8.5 and 10 Å. Imidazole derivatives not containing a COOH group show strong inhibitory power for fatty acid cyclooxygenase as well as TX-SYN. Cyclooxygenase is also known to be a metallo enzyme containing iron. The presence of the COOH enhances inhibitor selectivity for TX-SYN.
12. The procedures of preparation of Gel A-G were described in a separate paper submitted to *Bull. Korean Chem. Soc.* Volume 13, p. 221(1992).
13. P. W. Manley, N. M. Allanson, R. G. Booth, and DP. Tuffin, *J. Med. Chem.*, **30**, 1588 (1987).
14. (a) CA. Mullin and B. D. Mammock, *Arch. Biochem. Biophys.* **216**, 423 (1982); (b) K. Pommerenig, M. Kuhn, W. Jung, and M. Benes, *Int. J. Biol. Macromol.*, **1**, 79 (1979).
15. (a) T. Yoshimoto and S. Yamamoto, *Methods in Enzymology* **86**, pp. 106 (1982); (b) F. F. Sun, *Biochem. Biophys. Res. Commun.*, **74**, 1432 (1977).
16. P. Mohr, and K. Pommerenig, *Affinity chromatography, A series of Monographs Volume 33* (1985).
17. MM. Bradford, *Anal Biochem.* **72**, 248 (1976).
18. For the synthesis of A-1, See "Small Molecule Agents that Inhibit or Enhance Thromboxane Synthase Activity" Submitted to *Eur. J. Pharmacology* (Niels H. Andersen and Jaekool Rhee), See ref. 1.
19. Benzylimidazole is also known to be a weak inhibitor of TX-SYN with a demonstrated moderate affinity for TX-SYN.
20. Sheep seminal vesicles were obtained from Dr. Robert Solomon. Department of Chemistry, Case Western University, Cleveland, U.S.A.

## Structure and Bonding of Perovskites $\text{A}(\text{Cu}_{1/3}\text{Nb}_{2/3})\text{O}_3$ (A=Sr, Ba and Pb) and Their Series of Mixed Perovskites

Hyu-Bum Park, Hwang Huh<sup>†</sup>, and Si-Joong Kim\*

Department of Chemistry, Korea University, Seoul 136-701

<sup>†</sup>Department of Chemistry, Ul-San University, Ul-San 680-749. Received July 29, 1991

Some perovskites  $\text{A}(\text{Cu}_{1/3}\text{Nb}_{2/3})\text{O}_3$  (A= $\text{Sr}^{2+}$ ,  $\text{Ba}^{2+}$  and  $\text{Pb}^{2+}$ ) and their series of mixed perovskites have been prepared by solid state reaction. Single perovskite phase was obtained in Sr or Ba rich samples, but pyrochlore phase was found in Pb rich samples. The stability of perovskite phase is dependent on the ionicity of bonding as well as the tolerance factor. All the obtained perovskites have tetragonal symmetry distorted by Jahn-Teller effect of  $\text{Cu}^{2+}$ . In the case of  $\text{Sr}(\text{Cu}_{1/3}\text{Nb}_{2/3})\text{O}_3$ , some superlattice lines caused by threefold enlarging of fundamental unit cell were observed. And, the symmetry of B site octahedron and the bonding character of B-O bond have been studied by IR, ESR and diffuse reflection spectroscopy. It appeared that the symmetry and the bonding character are influenced by such factors as the size and the basicity of A cation.

### Introduction

Many compounds with the general formula  $\text{ABO}_3$  having perovskite structures have been prepared and studied by

many investigators.<sup>1-4</sup> These compounds exhibit many interesting physical properties such as ferroelectricity, piezoelectricity, and larger variation in electric and magnetic behaviours.<sup>5-8</sup> These properties depend on not only the crystal

structure, but also the properties of A and B ions. In oxide perovskites, although the bonding character is predominantly ionic, there exists a secondary covalent bonding between B ion and oxide ion, and also the B ion interacts with A ion through oxide ion. The electric and magnetic properties are directly related to the bonding properties.<sup>5,9</sup> To understand the properties of perovskites, hence, it is necessary to know the interaction between A ion and B ion.

In this research, we carried out a detailed study to understand the influences of A site ion on the structure and the bonding character for the perovskites  $A(\text{Cu}_{1/3}\text{Nb}_{2/3})\text{O}_3$  ( $A = \text{Sr}^{2+}$ ,  $\text{Ba}^{2+}$  and  $\text{Pb}^{2+}$ ) and their series of mixed perovskites by XRD, IR, ESR, and diffuse reflection spectroscopy.

### Experimental

All samples were prepared by solid state reaction. Each sample was prepared by mixing  $\text{SrCO}_3$ ,  $\text{BaCO}_3$ ,  $\text{PbO}$ ,  $\text{Nb}_2\text{O}_5$  and  $\text{Cu}(\text{CH}_3\text{COO})_2 \cdot \text{H}_2\text{O}$  through ball milling. The mixed powders were reacted at 850–950°C for 3 hr in alumina crucible and pressed into pellets, then further reacted at 950–1100°C for 5–50 hr. Pellets containing  $\text{PbO}$  were covered with the same compositional powders to minimize  $\text{PbO}$  evaporation at a given synthetic condition. The compositions of the final samples were checked by X-ray energy dispersive spectroscopy.

The phases and the crystal structures of the obtained samples were identified by X-ray powder diffraction with  $\text{Cu K}\alpha$  radiation and the lattice parameters were calculated by Cohen's method. IR spectra were obtained in the range of 1000–400  $\text{cm}^{-1}$  by employing BOMEM MB-100 spectrometer as  $\text{KBr}$  pellet. Diffuse reflection spectra of powdered samples were measured on Shimadzu UV-3100S spectrometer. To investigate the symmetry of  $\text{CuO}_6$  and the covalency of  $\text{Cu-O}$  bond, ESR spectra were recorded in X-band frequency region by Bruker ER 200D-SRC at room temperature.

### Results and Discussion

The perovskite ( $\text{ABO}_3$ ) structure is regarded as close-packed  $\text{AO}_3$  layers with B cations in octahedral holes. The A ions are coordinated by twelve oxide ions and B ions by six. In general, the stability of perovskite structure can primarily be estimated by geometrical consideration and described in terms of a tolerance factor,  $t$ , defined as

$$t = (r_A + r_O) / 1.414 (r_B + r_O)$$

where  $r_A$ ,  $r_B$  and  $r_O$  are ionic radii of the respective ions. In an ideal cubic perovskite where the ions are just touching one another, the tolerance factor is unity. When the tolerance factor is around unity, the perovskite phase is stable. The tolerance factors calculated using Shannon's<sup>10</sup> ionic radii are close to 1.0 [ $\text{Sr}(\text{Cu}_{1/3}\text{Nb}_{2/3})\text{O}_3$  [SCN],  $t = 0.97$ ;  $\text{Ba}(\text{Cu}_{1/3}\text{Nb}_{2/3})\text{O}_3$  [BCN],  $t = 1.03$ ;  $\text{Pb}(\text{Cu}_{1/3}\text{Nb}_{2/3})\text{O}_3$  [PCN],  $t = 0.99$ ]. All the samples, therefore, are expected to form perovskite phases.

**XRD.** XRD patterns in Figure 1 show that SCN and BCN form single perovskite phases, but PCN is composed of  $\text{Pb}_3\text{Nb}_4\text{O}_{13}$  (pyrochlore),  $\text{PbO}$  (yellow) and  $\text{CuO}$  (tenorite). It is well known that several Pb-based perovskites are difficult to prepare because of formation of pyrochlore phase.<sup>11,13</sup> From studies of formation of Pb-based perovskite, Halliyal

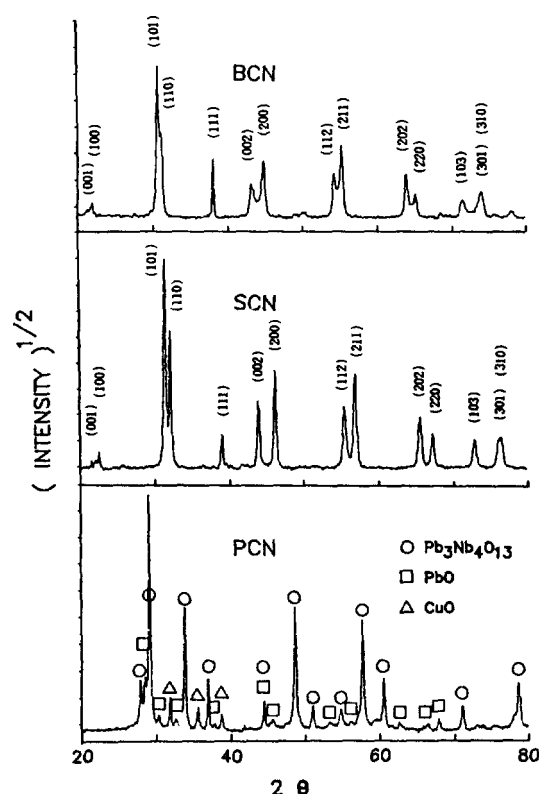
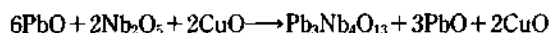


Figure 1. XRD patterns of  $\text{Ba}(\text{Cu}_{1/3}\text{Nb}_{2/3})\text{O}_3$  (BCN),  $\text{Sr}(\text{Cu}_{1/3}\text{Nb}_{2/3})\text{O}_3$  (SCN) and  $\text{Pb}(\text{Cu}_{1/3}\text{Nb}_{2/3})\text{O}_3$  (PCN).

and co-workers<sup>11</sup> have reported that an important factor to be considered in preparing those perovskites is the electronegativity difference between cation and anion, and that those Pb-based perovskites can be prepared by small addition of some other perovskites having higher ionicity. Since the difference of electronegativity in  $\text{Pb-O}$  is smaller than that in  $\text{Sr-O}$  and  $\text{Ba-O}$ , it would be difficult for the PCN composition to form perovskite phase. The XRD pattern of PCN can be analyzed as a result of the following reaction similar to that reported in the other papers.<sup>12,13</sup>



The XRD patterns of SCN and BCN show the tetragonal distortion of crystal lattice, and SCN especially shows larger distortion. It seems that the tetragonal distortion is caused by Jahn-Teller distortion of  $\text{Cu}^{2+}$  in  $\text{BO}_6$  octahedron. In the case of SCN ( $t = 0.97$ ), small  $\text{Sr}^{2+}$  can cause co-operative buckling of the corner-shared octahedron which enlarges the unit cell,<sup>14</sup> and the buckling can distort the closed packing of ions in crystal lattice. The larger distortion in SCN would take place as a consequence of the buckling and it seems that this distortion would enhance the structural stability.

The phase diagrams of three systems,  $(1-x)\text{BCN}-x\text{SCN}$ ,  $(1-x)\text{PCN}-x\text{BCN}$ , and  $(1-x)\text{PCN}-x\text{SCN}$ , are presented in Figure 2. The series  $(1-x)\text{BCN}-x\text{SCN}$  forms a complete solid solution of perovskite phase, but  $(1-x)\text{PCN}-x\text{BCN}$  and  $(1-x)\text{PCN}-x\text{SCN}$  do not form solid solution in the region of higher  $\text{Pb}^{2+}$  content with the formation of undesired pyrochlore ( $\text{Pb}_3\text{Nb}_4\text{O}_{13}$ ). All the obtained perovskite phases are tetragonal due to the cooperative Jahn-Teller distortion of

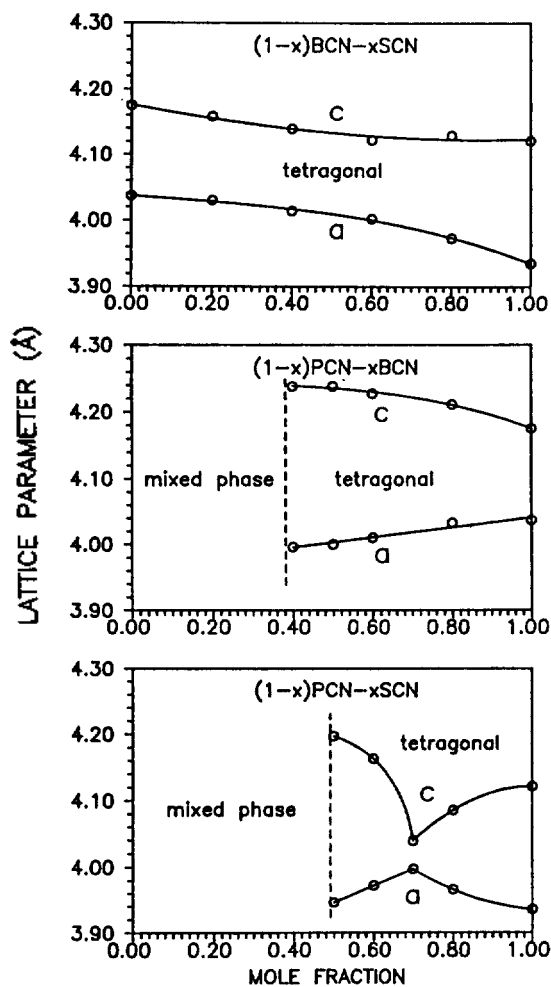


Figure 2. Phase diagrams of  $(1-x)\text{BCN}-x\text{SCN}$ ,  $(1-x)\text{PCN}-x\text{BCN}$  and  $(1-x)\text{PCN}-x\text{SCN}$ .

$\text{Cu}^{2+}$ , which might be an important factor determining the crystal symmetry. As  $\text{Ba}^{2+}$  of BCN is substituted for  $\text{Pb}^{2+}$ , the tetragonality is increased. This increase of tetragonality seems to be caused by inert pair effect of  $\text{Pb}^{2+}$ . In some compounds, the  $6s^2$  electrons of  $\text{Pb}^{2+}$  are stereochemically active, since this electron pair is not in spherically symmetrical orbital but stick out to one side of the  $\text{Pb}^{2+}$  ion.<sup>9</sup> The inert pair is able to bring about a distortion of coordination polyhedra of the metal ion, furthermore, a distortion of the crystal structure.<sup>9,15,16</sup> Assuming that there is the inert pair effect, the tetragonal distortion in  $\text{Pb}^{2+}$  rich samples can be promoted by the addition of co-operative inert pair effect to Jahn-Teller effect.  $(1-x)\text{PCN}-x\text{SCN}$  series exhibits a point of lower tetragonality near  $x=0.7$ , which seems to be difficult to be interpreted. It is thought that another factor which does not exist in  $(1-x)\text{BCN}-x\text{SCN}$  and  $(1-x)\text{PCN}-x\text{BCN}$  may play an important role in  $(1-x)\text{PCN}-x\text{SCN}$ .

If there are more than one kind of ion in B site, the ordering of B site ions is possible. It has been known that the ordering of B ions is more probable when a large difference exists in size and charge between the B ions.<sup>17,18</sup> Superlattice lines of BCN and SCN were investigated for the samples reacted at  $1100^\circ\text{C}$  and annealed at  $800^\circ\text{C}$  to improve the ordering. In Figure 3, SCN shows some superlattice lines

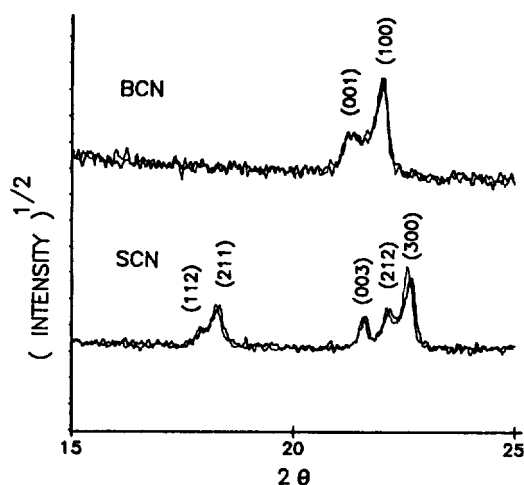


Figure 3. XRD patterns of SCN and BCN obtained by heat treatment at  $1100^\circ\text{C}$  for 50 hr (thin line) and additional annealing at  $800^\circ\text{C}$  for 15 hr (thick line).

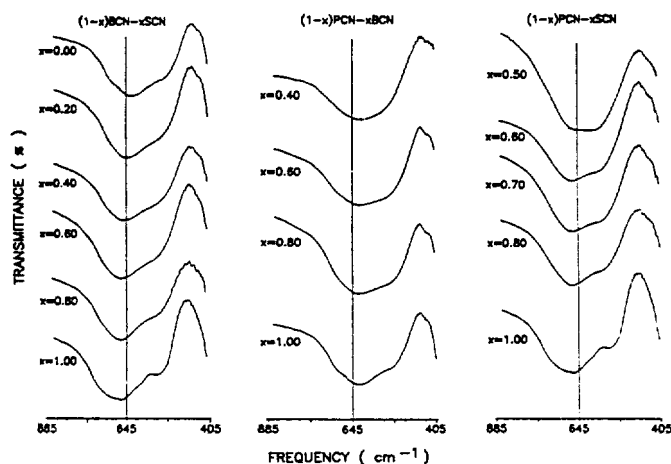


Figure 4. IR spectra of  $(1-x)\text{BCN}-x\text{SCN}$ ,  $(1-x)\text{PCN}-x\text{BCN}$  and  $(1-x)\text{PCN}-x\text{SCN}$ .

[[112], (211), and (212)] due to threefold enlarging of fundamental unit cell, but BCN does not show noticeable superlattice lines under the same X-ray diffraction condition. Since the A site is occupied entirely by  $\text{Sr}^{2+}$  and the B site is composed of two different ions ( $1/2\text{Cu}^{2+}$  and  $2/3\text{Nb}^{5+}$ ) in SCN, and the differences in charge and size between  $\text{Cu}^{2+}$  and  $\text{Nb}^{5+}$  are enough to cause an ordering, it can be suggested that the threefold enlarging of unit cell takes place as a result of the 1:2 ordering of B site ions ( $\text{CuNbNbCuNbNb}\dots$ ).

**IR Spectra.** The vibrational spectra of perovskites have been frequently described as the internal vibration of the octahedron containing highly charged and small B ion because of relatively weak A-O bond.<sup>19-21</sup> In  $\text{A}(\text{Cu}_{1/3}\text{Nb}_{2/3})\text{O}_3$  compounds, the Nb-O bonding is expected to be stronger and more covalent than the Cu-O bonding, and thus the  $\text{NbO}_6$  group is regarded as a molecular unity. Blasse and Corsmit<sup>22</sup> have reported that the stretching frequencies of  $\text{NbO}_6$  group for some perovskites are ranged between 590 and  $660\text{ cm}^{-1}$ , and also Husson and co-workers<sup>23</sup> have repor-

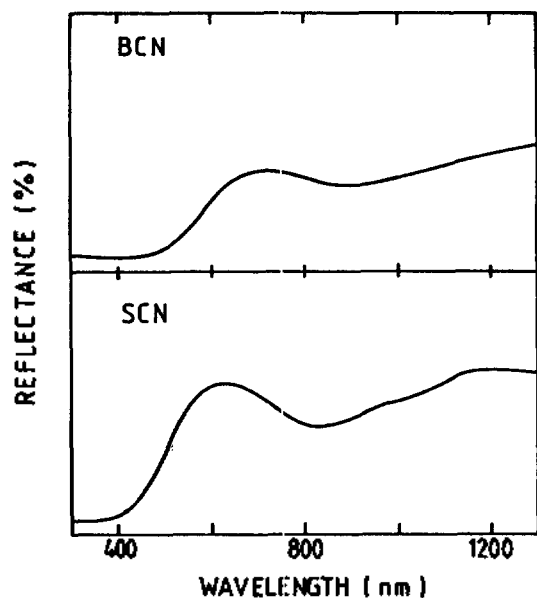


Figure 5. Diffuse reflection spectra of BCN and SCN.

ted that the stretching frequency of  $\text{NbO}_6$  in  $\text{Pb}(\text{Mg}_{1/3}\text{Nb}_{2/3})\text{O}_3$  is  $600\text{ cm}^{-1}$ . In three series, IR absorptions are observed between  $540$  and  $670\text{ cm}^{-1}$  (see Figure 4).

The  $\text{BO}_6$  octahedron has 15 internal degrees of freedom or normal vibrations:  $A_g + E_g + 2T_{1u} + T_{2g} + T_{2u}$ . According to group theoretical consideration, the two  $T_{1u}$  modes are IR active and correspond to the stretching and the bending motions in  $\text{BO}_6$  octahedron. Since the crystal symmetry for each sample is tetragonal, there is quite a possibility that the  $\text{NbO}_6$  octahedron is tetragonally distorted. If  $O_h$  symmetry of  $\text{NbO}_6$  is lowered to  $D_{4h}$ , it is expected that the  $T_{1u}$  modes are split into  $A_{2u}$  and  $E_u$  modes. The stretching motions corresponding to  $E_u$  are the vibrations of shorter Nb-O bonds in elongated octahedron, and that corresponding to  $A_{2u}$  is the vibration of longer Nb-O bond. Most of IR spectra in Figure 4 virtually show strong bands ( $E_u$ ) around  $650\text{ cm}^{-1}$  and shoulders ( $A_{2u}$ ) at lower frequencies.

In  $(1-x)\text{BCN}-x\text{SCN}$ , the stretching frequency of Nb-O bond increases gradually from  $x=0.00$  to  $1.00$ . This increase may be ascribed to the size effect of A site ion. Small  $\text{Sr}^{2+}$  compresses the B site octahedron and thus the B-O bond length is shortened. Therefore, the gradual substitution of  $\text{Sr}^{2+}$  for  $\text{Ba}^{2+}$  of BCN results in the increase of stretching frequency. The IR spectrum of SCN shows the largest band splitting, which indicates the most distorted  $\text{NbO}_6$  octahedron. The splitting degree between maximum ( $E_u$ ) and shoulder ( $A_{2u}$ ) increases with increasing  $\text{Sr}^{2+}$  content. This increase of band splitting is in good agreement with the increase of tetragonal distortion of crystal lattice observed by XRD.

IR spectra of  $(1-x)\text{PCN}-x\text{BCN}$  and  $(1-x)\text{PCN}-x\text{SCN}$  show only a small shift of the stretching band of Nb-O. But, the IR bands of  $(1-x)\text{PCN}-x\text{SCN}$  are positioned at higher frequencies than those of  $(1-x)\text{PCN}-x\text{BCN}$ , which implies that the size of A site ion has an important effect on the B-O bond strength. In  $(1-x)\text{PCN}-x\text{BCN}$ , the splitting degree of IR bands decreases with increasing  $\text{Pb}^{2+}$  content, even though the tetragonality of unit cell increases. In addi-

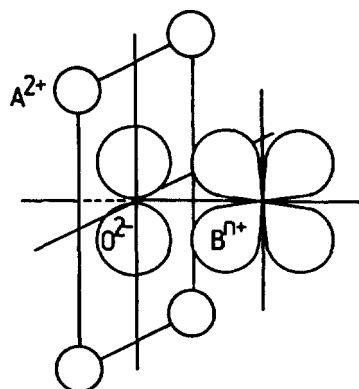


Figure 6. Anion coordination in perovskite structure.

tion, the band splitting in IR spectra continuously decreases with increasing  $\text{Pb}^{2+}$  content, although the phase diagram of  $(1-x)\text{PCN}-x\text{SCN}$  shows a minimum point of tetragonality near  $x=0.70$ . From these results, it turns out that the symmetry of  $\text{NbO}_6$  is independent of the crystal symmetry in  $\text{Pb}^{2+}$  rich region and the behavior of  $\text{Pb}^{2+}$  in these perovskites is different from that of  $\text{Sr}^{2+}$  or  $\text{Ba}^{2+}$ .

**Diffuse Reflection Spectra.** Diffuse reflection spectra were measured to know variation of the band gap in compounds and the  $d-d$  transition energy of  $\text{Cu}^{2+}$ . It is well known that the magnitude of band gap depends on ionicity of bonding in solid.<sup>9</sup> Representative diffuse reflection spectra of BCN and SCN are shown in Figure 5. Absorption edges, which are designated as the wavelength having maximum derivatives of reflectance, are positioned at  $510\text{ nm}$  for SCN and at  $577\text{ nm}$  for BCN. Absorptions due to  $d-d$  transition of  $\text{Cu}^{2+}$  are also observed at  $830\text{ nm}$  (and near  $1000\text{ nm}$  as shoulder) for SCN and at  $895\text{ nm}$  for BCN. SCN shows typical spectrum of  $\text{Cu}^{2+}$  ion in elongated octahedral field, but BCN does not show any remarkable shoulder.

It is assumed that the absorption edges observed in the range of  $510-660\text{ nm}$  are due to absorption of niobate group and are originated from charge transfer transition in which an electron is transferred from the highest filled molecular orbital (localized on the oxide ions) to the lowest empty molecular orbital (localized on the niobium ion). In perovskite structure, the oxide ions are coordinated by B ions and by a square of four A ions at larger distances, this square being perpendicular to the collinear array B-O-B<sup>2n+</sup> (see Figure 6). The occupied oxygen  $2p$  orbitals are situated in the square composed of four A site ions and the empty  $t_{2g}$  orbital of  $\text{Nb}^{5+}$  is coordinated to the  $2p$  orbital of oxide ion. Hence, by considering the fact that the  $2p$  orbital can be directed toward A site ions, it is reasonable for the absorption edge to depend on A site ion.

Figure 7 illustrates that the absorption edge depends on the composition of A site. In  $(1-x)\text{BCN}-x\text{SCN}$  series, the absorption edge decreases with increasing  $\text{Ba}^{2+}$  content in A site and the two systems containing  $\text{Pb}^{2+}$  also show the decrease of absorption edge with increasing  $\text{Pb}^{2+}$  content. The trend of absorption edge energy is, on the whole,  $\text{Pb} < \text{Ba} < \text{Sr}$ . This trend is reverse to the basicity of A site ions. If the A ion is able to give more electron cloud to oxide ion, the Nb-O bond becomes more covalent and the charge

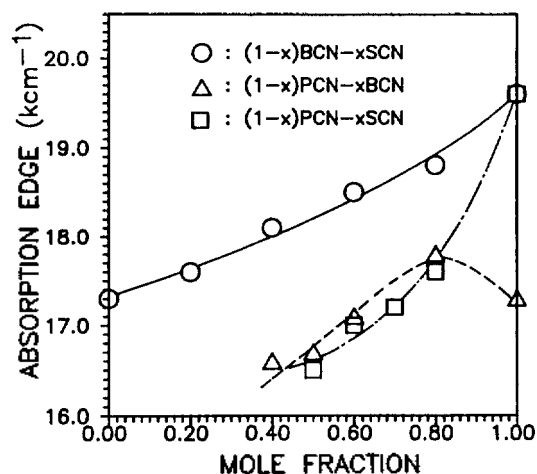


**Figure 7.** Variation of absorption edges for (1-x)BCN-xSCN, (1-x)PCN-xBCN and (1-x)PCN-xSCN.

transfer transition from  $O^{2-}$  to  $Nb^{5+}$  can be facilitated. More basic  $Pb^{2+}$  ion, therefore, shifts absorption edge to lower frequency.

**ESR Spectra.** ESR spectra were recorded to observe the symmetry of  $CuO_6$  and the covalency in Cu-O bonding. All the obtained ESR spectra showed nearly isotropic shapes, which revealed symmetrical surroundings of  $Cu^{2+}$ , with the exception of SCN. The anisotropy of SCN seems to be ascribed to the lower symmetry caused by larger Jahn-Teller distortion. In IR spectrum of SCN, the largest band splitting is also observed. Therefore, it may be inferred that in the case of SCN both  $Cu^{2+}$  and  $Nb^{5+}$  have more distorted surroundings. The  $g$  factors of three series are ranged in 2.20-2.15 (Table 1), which agree to the value 2.192 reported by Coffman<sup>25</sup> for  $Cu^{2+}$  doped MgO.

In (1-x)BCN-xSCN, the variation of  $g$  factor for Cu-O bonding is relatively small. The Cu-O in SCN is more covalent than that in BCN, which can be explained by the buckling effect. The  $CuO_6$  octahedron is more compressed by smaller  $Sr^{2+}$ , and thus the orbitals between  $Cu^{2+}$  and  $O^{2-}$  is much more overlapped. However, the  $g$  factor in (1-x)PCN-xBCN series largely decreases with the increase of  $Pb^{2+}$  content.  $Pb^{2+}$  favors covalent bonding than  $Ba^{2+}$  ion and can give more electron cloud to oxygen ions and thus the covalency of Cu-O might be increased as the increase

**Table 1.**  $g$  Factor and  $\Delta H_{pp}(G)$ , of (1-x)BCN-xSCN, of (1-x)PCN-xBCN at Room Temperature

$x$	(1-x)BCN-xSCN		(1-x)PCN-xBCN		(1-x)PCN-xSCN	
	$g$	$\Delta H_{pp}$	$g$	$\Delta H_{pp}$	$g$	$\Delta H_{pp}$
0.00	2.20	325	-	-	-	-
0.20	2.20	285	-	-	-	-
0.40	2.20	270	2.15	645	-	-
0.50	-	-	2.16	579	2.17	610
0.60	2.20	260	2.16	475	2.18	520
0.70	-	-	-	-	2.19	395
0.80	2.19	265	2.18	390	2.19	335
1.00	2.18	260	2.20	325	2.18	260

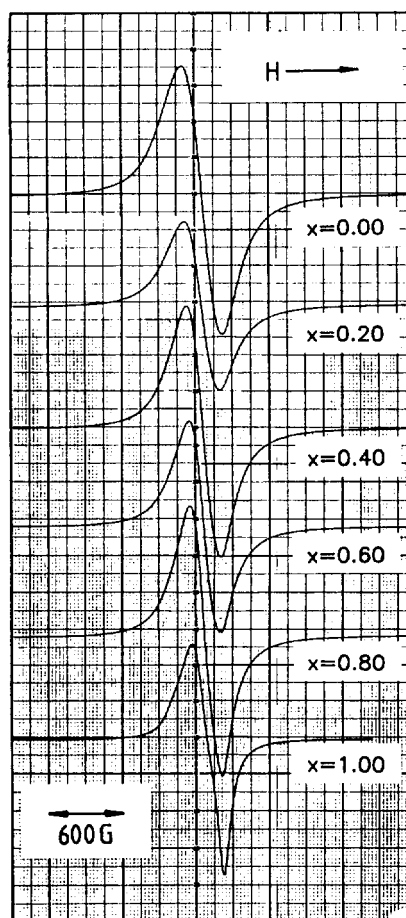


**Figure 8.** X-band ESR spectra of (1-x)BCN-xSCN at room temperature.

of  $Pb^{2+}$  content. The effect of basicity of  $Pb^{2+}$  on the increase of covalency of Cu-O is stronger than that of the buckling of  $Sr^{2+}$ . On the other hand, in (1-x)PCN-xSCN system a small decrease of  $g$  factor was observed. The buckling effect is reduced with increasing  $Pb^{2+}$  content, since  $Pb^{2+}$  (1.49 Å) is larger than  $Sr^{2+}$  (1.44 Å). In (1-x)PCN-xSCN, the effect of basic  $Pb^{2+}$  on  $g$  factor might be compensated by the reduced buckling.

By considering peak-to-peak linewidth ( $\Delta H_{pp}$ ) values tabulated in Table 1, the  $\Delta H_{pp}$  considerably increases along with the decrease of  $g$  factor, as the  $Pb^{2+}$  content in A site increases. Such a phenomena could be explained by the enhancement of electron delocalization in the Cu-O bond due to the increment of covalency.

## Conclusions

The stability of perovskite phase is related to both the tolerance factor and the difference of electronegativity between cation and anion in compound. All the crystal symmetry of obtained perovskites were tetragonal. The main factors determining crystal symmetry are Jahn-Teller distortion of  $Cu^{2+}$  and inert pair effect of  $Pb^{2+}$ . In SCN, some superlattice lines caused by three fold enlarging of unit cell were observed.

The stretching frequency of Nb-O bond depended on the

size of A ion and the symmetry of NbO<sub>6</sub> on both the crystal symmetry and the property of A ion. The absorption edge decreased, as the basicity of A ion was increased and the size of A ion was decreased. ESR spectra of Cu<sup>2+</sup> showed nearly isotropic shapes with the exception of SCN and the covalency of Cu-O bond depended on the basicity and the size of A ion. The important factors, which affect the bonding character of B-O and the symmetry of BO<sub>6</sub> octahedron, were the size and the basicity of A ion.

**Acknowledgement.** This work was financially supported by Korea Science and Engineering Foundation in 1991.

### References

1. G. Blasse, *J. Inorg. Nucl. Chem.*, **27**, 993 (1965).
2. E. Takayama-Muromachi and A. Navrotsky, *J. Solid State Chem.*, **72**, 244 (1988).
3. K. Hayashi, H. Noguchi, and M. Ishii, *Mat. Res. Bull.*, **21**, 401 (1986).
4. T. Nakamura and J. H. Choy, *J. Solid State Chem.*, **20**, 233 (1977).
5. R. C. Buchanan, "Ceramic Materials for Electronics", Marcel Dekker, Inc., New York, U.S.A. 1986.
6. P. Ganguly, N. Y. Vasanthacharya, C. N. R. Rao, and P. P. Edwards, *J. Solid State Chem.*, **54**, 400 (1984).
7. B. Jaffe, W. R. Cook Jr., and H. Jaffe, "Piezoelectric Ceramics", Academic Press, London, England, 1971.
8. A. W. Sleight and J. F. Weiher, *J. Phys. Chem. Solids*, **33**, 679 (1972).
9. A. R. West, "Solid State Chemistry and its Applications", John Wiley & Sons Ltd., New York, U.S.A. 1984.
10. R. D. Shannon and C. T. Prewitt, *Acta Cryst.*, **B25**, 925 (1969).
11. A. Halliyal, U. Kumar, R. E. Newnham, and L. E. Cross, *Am. Ceram. Soc. Bull.*, **66**, 671 (1987).
12. M. Lejeune and J. P. Boilot, *Ceramics International*, **8**, 99 (1982).
13. S. L. Swartz and T. R. Shrout, *Mat. Res. Bull.*, **17**, 1245 (1982).
14. G. Blasse, *J. Inorg. Nucl. Chem.*, **35**, 1347 (1975).
15. G. Shirane, R. Pepinsky, and B. C. Frazer, *Acta Cryst.*, **9** 131 (1956).
16. J. A. Alonso and I. Rasines, *J. Phys. Chem. Solids*, **49**, 385 (1988).
17. F. Galasso, L. Katz, and R. Ward, *J. Am. Chem. Soc.*, **81**, 820 (1959).
18. F. Galasso and W. Darby, *J. Phys. Chem.*, **66**, 131 (1962).
19. N. Ramadass, J. Gopalakrishnan, and M. V. C. Sastri, *J. Inorg. Nucl. Chem.*, **40**, 1453 (1978).
20. J. T. Last, *Phys. Rev.*, **105**, 1740 (1957).
21. A. F. Corsmit, H. E. Hoefdraad, and G. Blasse, *J. Inorg. Nucl. Chem.*, **34**, 3401 (1974).
22. G. Blasse and A. F. Corsmit, *J. Solid State Chem.*, **10**, 39 (1974).
23. E. Husson, L. Abello, and A. Morell, *Mat. Res. Bull.*, **25**, 539 (1990).
24. G. Blasse and A. F. Corsmit, *J. Solid State Chem.*, **6**, 513 (1973).
25. R. E. Coffman, *J. Chem. Phys.*, **48**, 609 (1968).

## Infrared Spectra and Electrical Conductivity of The Solid Solutions X MgO+(1-X) $\alpha$ -Nb<sub>2</sub>O<sub>5</sub>; 0.01≤X≤0.09

Zin Park, Jong Sik Park, Dong Hoon Lee, Jong Ho Jun<sup>†</sup>,  
Chul Hyun Yo, and Keu Hong Kim\*

Department of Chemistry, Yonsei University, Seoul 120-749

<sup>†</sup>Department of Biochemistry, Kon-Kuk University, Chungju 380. Received August 10, 1991

Changes in network structures of  $\alpha$ -Nb<sub>2</sub>O<sub>5</sub> in the X MgO+(1-X)  $\alpha$ -Nb<sub>2</sub>O<sub>5</sub> solid solutions occurring as the MgO doping level (X) was varied were investigated by means of infrared spectroscopy and X-ray analysis. X-ray diffraction revealed that all the synthesized specimens have the monoclinic structure. The FT-IR spectroscopy showed that the system investigated forms the solid solutions in which Mg<sup>2+</sup> ions occupy the octahedral sites in parent crystal lattice. Electrical conductivities were measured as a function of temperature from 600 to 1050°C and P<sub>O<sub>2</sub></sub> from 1×10<sup>-5</sup> to 2×10<sup>-1</sup> atm. The defect structure and conduction mechanism were deduced from the results. The 1/n value in  $\sigma \propto P_{O_2}^{1/n}$  is found to be -1/4 with single possible defect model. From the activation energy (E<sub>a</sub>=1.67-1.73 eV) and the 1/n value, electronic conduction mechanism is suggested with a doubly charged oxygen vacancy.

### Introduction

The polymorphism of niobium pentoxide has been studied by several investigators. The  $\alpha$  form of Nb<sub>2</sub>O<sub>5</sub> is the most thermodynamically stable polymorph in the high tempera-

ture. The transition temperature of the  $\alpha$  form from the low temperature modification has been found to be approximately 830°C and the transition is irreversible<sup>1</sup>. The structure of  $\alpha$ -Nb<sub>2</sub>O<sub>5</sub> is derived from the ReO<sub>3</sub>-type structure. The crystal structure of  $\alpha$ -Nb<sub>2</sub>O<sub>5</sub> has been found to be monoclinic, space